ORGANOMETALLICS

Article

pubs.acs.org/Organometallics

Control of Olefin Hydroarylation Catalysis via a Sterically and Electronically Flexible Platinum(II) Catalyst Scaffold

Bradley A. McKeown,[†] Hector Emanuel Gonzalez,[‡] Thoe Michaelos,[§] T. Brent Gunnoe,*[,†] Thomas R. Cundari,*[,‡] Robert H. Crabtree,[§] and Michal Sabat[∥]

[†]Department of Chemistry, University of Virginia, Charlottesville, Virginia 22904, United States

[‡]Center for Advanced Scientific Computing and Modeling (CASCaM), Department of Chemistry and Energy Sciences Institute, University of North Texas, Denton, Texas 76203, United States

[§]Department of Chemistry and Energy Sciences Institute, Yale University, New Haven, Connecticut 06520, United States

[∥]Nanoscale Materials Characterization Facility, Materials Science and Engineering Department, University of Virginia, Charlottesville, Virginia 22904, United States

Supporting Information

ABSTRACT: Pt^{II} complexes supported by dipyridyl ligands have been demonstrated to catalyze olefin hydroarylation. Herein, studies on the influence of dipyridyl motif variation are reported. Increasing the chelate ring size of dipyridyl-ligated Pt^{II} complexes from five- to six-membered rings by replacing 4,4′-di-*tert*-butyl-2,2′-bipyridine with 2,2′-dipyridylmethane has been shown to increase catalytic activity and longevity for catalytic ethylene hydrophenylation. For 2,2′-dipyridyl ligands, the presence of methyl groups in the 6/6′-positions of the pyridyl rings reduces the extent of dialkylation to produce diethylbenzenes but also increases the rate of catalyst decomposition. Substituting the methylene spacer between the pyridyl rings of 2,2′-dipyridylmethane with more electron-withdrawing groups also reduces catalytic efficiency. The steric profile of Pt^{II} complexes with increased chelate ring size or substituents in the 6/6′-positions of the pyridyl rings provides a marked change in regioselectivity for ethylene hydroarylation using ethylbenzene as well as the linear to branched selectivity for the hydrophenylation of propylene.

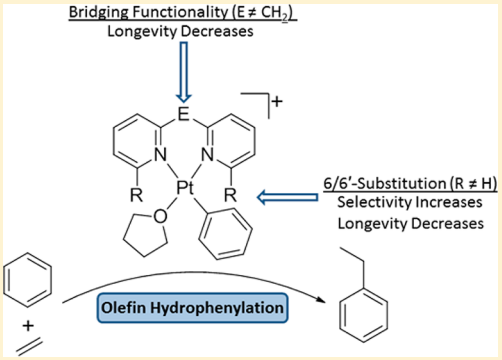

INTRODUCTION

The direct and selective functionalization of hydrocarbons by C−H bond activation and subsequent C−C bond formation remains challenging but has the potential to become a valuable tool for organic synthesis.[1] For example, the conversion of olefins and arenes to alkyl arenes is an important industrial reaction.[2] Current methods for alkyl arene production utilize acids (Lewis and/or Brønsted) to catalyze the net addition of an aromatic C−H bond across an olefin C═C bond (olefin hydroarylation) by a Friedel−Crafts pathway.[3] Despite being widely employed, these processes have limitations that result from the intermediacy of carbocations.[1b,4] For example, acid catalysts are highly selective for the formation of Markovnikov products when substituted olefins are used. In addition, directing groups on the arene dictate regioselectivity, and in cases of "non-functional" groups (e.g., alkyl groups), little regioselectivity can be achieved. Alkylated arene products are typically more reactive than starting arenes, and polyalkylation at high substrate conversion is problematic. While zeolites have provided improvement over traditional Friedel−Crafts catalysts,[2b,5] they operate by the same fundamental mechanism. A transition-metal-mediated pathway that combines olefin insertion into metal−aryl bonds and aromatic C−H activation provides a route to alkyl arenes that is complementary to acid-catalyzed processes and offers the potential to overcome the limitations of traditional methodologies.[1b,4]

Examples of olefin hydroarylation by a non-acid-catalyzed mechanism to yield alkyl arenes are limited and often require chelate assistance[6] or substrates activated by heterofunctional groups.[7] The use of unactivated substrates (e.g., benzene and ethylene) for olefin hydroarylation has been realized with Ru, Ir, and Pt catalyst precursors.[4,8] In order to develop improved catalyst systems, it is necessary to understand how alterations of the catalyst's electronic and steric properties influence selectivity. However, few detailed studies delineating structure/activity relationships are available to guide new catalyst design.[4a,9]

Platinum has emerged as a promising candidate for catalytic olefin hydroarylation, with established precedent for metal-mediated olefin insertion and aromatic C−H activation[10] but inefficient oligomerization/polymerization.[11] Examples of olefin hydroarylation using Pt^{II} catalyst precursors have been reported,[8b−d,9b,12] but mechanistic evidence supporting a non-

Received: May 3, 2013
Published: June 28, 2013

Scheme 1. Proposed Catalytic Cycle for Ethylene Hydrophenylation by Cationic Bipyridyl-Supported Pt^{II} Complexes[a]

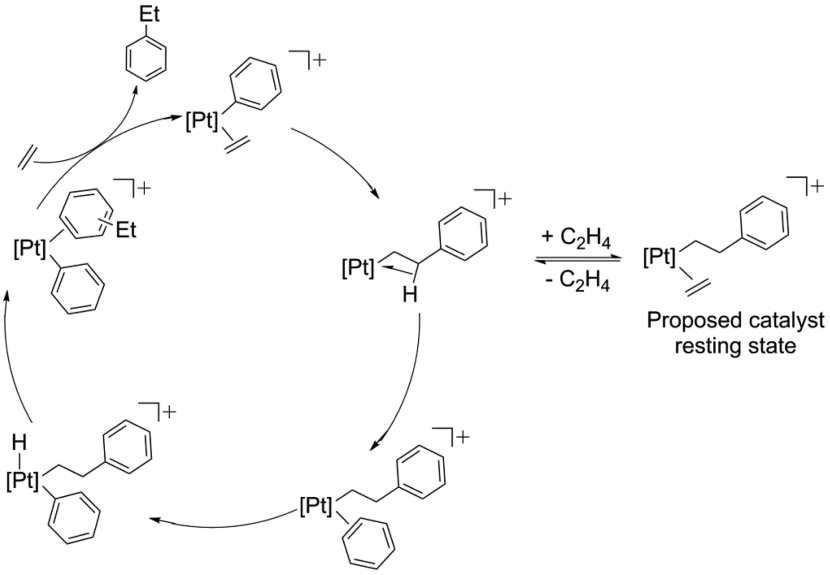

[a][Pt] = $[(N\sim N)Pt]^+$ and N∼N = ^{t}bpy, dpm.

acid-catalyzed pathway has been disclosed for only two complexes.[8c,9b−d] Goldberg and co-workers reported a Pt^{II} catalyst precursor ligated by a (pyridyl)pyrrolide ligand for which mechanistic studies are consistent with a pathway that incorporates olefin insertion into a Pt−aryl bond and subsequent activation of an aromatic C−H bond.[8c] Additionally, we have reported studies of ethylene hydrophenylation catalyzed by $[(N\sim N)Pt(Ph)(THF)][BAr'_4]$ (N∼N = 4,4′-di-*tert*-butyl-2,2′-bipyridine (^{t}bpy), 2,2′-dipyridylmethane (dpm); Ar′ = 3,5-$(CF_3)_2$-C_6H_3) that support a similar catalytic cycle (Scheme 1).[9b−d]

The bipyridyl framework is easily modified and presents an opportunity to establish structure/activity relationships. In a previous study, the 4,4′-substituents of the 2,2′-bipyridyl ligand were modified to probe the influence of electron-donor ability on catalyst selectivity without alteration of the catalyst steric profile.[9d] It was demonstrated that, by varying the donor ability of the 2,2′-bipyridyl ligand, the metal center can be attenuated to bias the formation of ethylbenzene versus styrene. In addition to electronic perturbations, we found that expansion of the dipyridyl ligand from a five- to six-membered chelate (i.e., using dpm in place of ^{t}bpy) provides an enhancement of catalyst activity and longevity.[9c] Recent work by Puddephatt et al. has also examined the influence of dipyridyl chelate ring size on the reactivity and selectivity of Pt^{II} alkyl complexes for arene C−H activation, H/D exchange, and oxidative addition reactions.[13] Diethylbenzenes constitute a significant portion (∼20%) of the total alkyl arene products using bipyridyl- and dipyridylmethane-ligated Pt^{II} catalyst precursors and likely result from aromatic C−H activation competing with ethylbenzene dissociation.[9b] We hypothesized that increased steric congestion around the Pt center might facilitate ethylbenzene displacement and provide increased selectivity for monoalkylated products. Moreover, we considered that steric perturbations about the Pt center could have an effect on the regioselectivity of α-olefin hydroarylation (i.e., selectivity for Markovnikov versus anti-Markovnikov products). In this report, the impact of changes to the catalyst, including 6,6′-pyridyl substitution, chelate ring size, and the identity of the bridging pyridyl functionality on catalyst activity and selectivity is disclosed (Chart 1). The catalysis data for $[(dpm)Pt(Ph)(THF)][BAr'_4]$ have been previously reported, but we have included them in various tables and discussions for comparative purposes.[9c]

Chart 1. Generic Structure for Dipyridyl-Ligated Pt^{II} Complexes, Highlighting the Substituents Studied in This Report[a]

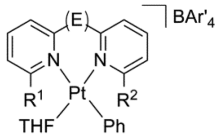

[a]E = CH_2, CH_2CH_2, C═O, NH, O; R^1, R^2 = H, Me.

RESULTS AND DISCUSSION

The complexes $(N\sim N)PtPh_2$ (N∼N = 6-methyl-2,2′-dipyridylmethane (Me-dpm, **1b**), 6,6′-dimethyl-2,2′-dipyridylmethane (Me_2-dpm, **1c**), 6,6′-dimethyl-2,2′-bipyridine (Me_2-bpy, **1d**), 1,2-bis(2-pyridyl)ethane (dpe, **1e**)) were prepared by reaction of the appropriate dipyridyl ligand with the binuclear platinum dimer $[Pt(Ph)_2(\mu\text{-}Et_2S)]_2$ (eq 1). Crystals suitable for an X-ray

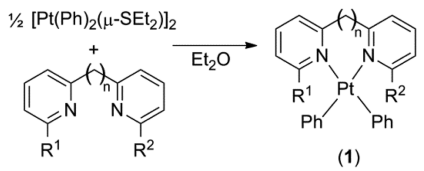

(1)

n = 1, R^1 = H, R^2 = Me (**1b**), 92% isolated yield
n = 1, R^1 = R^2 = Me (**1c**), 94% isolated yield
n = 0, R^1 = R^2 = Me (**1d**), 69% isolated yield
n = 2, R^1 = R^2 = H (**1e**), 76% isolated yield

diffraction study were obtained for complexes $(dpm)PtPh_2$ (**1a**) and **1c**,**e** (Figure 1 and Table 1). For the dpm complex **1a**, the N−Pt−N angle is increased by ∼9° to 86.0(3)° relative to the

dx.doi.org/10.1021/om400390e | Organometallics 2013, 32, 3903−3913

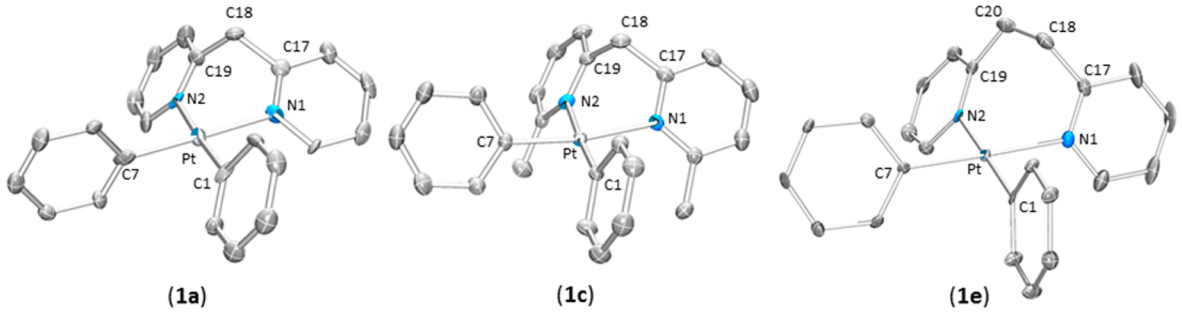

Figure 1. ORTEP drawings of complexes (dpm)Pt(Ph)$_2$ (**1a**), (Me$_2$-dpm)Pt(Ph)$_2$ (**1c**), and (dpe)Pt(Ph)$_2$ (**1e**) (50% probability; H atoms omitted for clarity).

Table 1. Comparison of Selected Bond Lengths and Angles among the Complexes (dpm)Pt(Ph)$_2$ (1a), (Me$_2$-dpm)Pt(Ph)$_2$ (1c), (dpe)Pt(Ph)$_2$ (1e), and (^{t}bpy)Pt(Ph)$_2$

	1a	1c	1e	(^{t}bpy)Pt(Ph)$_2$[a]
		Bond Lengths (Å)		
Pt–N1	2.133(7)	2.138(2)	2.124(7)	2.097(3)
Pt–N2	2.147(7)	2.131(2)	2.137(6)	2.097(3)
Pt–C1	2.018(8)	1.997(2)	2.016(7)	2.023(2)
Pt–C7	2.02(1)	1.998(2)	2.002(7)	2.023(2)
		Bond Angles (deg)		
N1–Pt–N2	86.0(3)	83.51(8)	87.8(2)	77.1(2)
N2–Pt–C1	176.9(4)	176.44(8)	178.6(3)	174.5(1)
N1–Pt–C1	91.1(3)	94.06(9)	92.4(3)	97.4(1)
C1–Pt–C7	88.2(4)	89.0(1)	89.3(3)	88.2(2)
C17–C18–C19	110.8(8)	110.1(2)		
C19–C20–C18–C17			53.6(1)	

[a]Crystallographic data from ref 14.

reported structure of (^{t}bpy)Pt(Ph)$_2$ (77.1(2)°).[14] The addition of methyl groups to the 6/6′-positions in complex **1c** results in an approximate 3° compression of the N–Pt–N bite angle (83.51(8)°) relative to **1a**. The additional methylene spacer to form a seven-membered chelate ring in complex **1e** has a small effect on the N–Pt–N angle (87.8(2)°) in comparison to the dipyridylmethane variants. For 2,2′-bipyridyl-ligated Pt complexes, the pyridyl rings reside approximately in the Pt square plane.[14,15] In contrast, the dpm complex **1a** adopts a pseudo-boat conformation that causes the pyridyl rings to be contorted out of the Pt square plane by ∼42° (average measurement of the N–Pt–N–C$_{2\text{-pyridyl}}$ torsion angles). The methyl groups in the 6/6′-positions of complex **1c** enhance this distortion with the pyridyl rings ∼52° out of planarity. Coordination of dpe to the PtPh$_2$ fragment results in the pyridyl rings being twisted out of the square plane by ∼58°. The 2,2′-bipyridyl complex (^{t}bpy)Pt(Ph)$_2$ possesses shorter Pt–N and longer Pt–C bond lengths in comparison to complexes **1a,c,e**, which is consistent with the ^{t}bpy ligand exerting a greater trans influence than dpm, 6,6′-dpm, or dpe.

The complexes [(N∼N)Pt(Ph)(THF)][BAr′$_4$] (**2b–e**) were prepared by protonation of **1b–e** with [H(Et$_2$O)$_2$][BAr′$_4$] at −70 °C in THF (eq 2). A suitable crystal of [(dpe)Pt(Ph)(THF)][BAr′$_4$] (**2e**) was obtained for an X-ray diffraction study (Figure 2). A search of the Cambridge Structural Database revealed only three examples of solid-state structures of Pt^{II}–THF complexes.[9d,16] Comparison of the previously reported structures of Pt^{II}–THF complexes suggests that dpe exerts the weakest *trans* influence with the Pt–O bond length increasing along the series dpe (2.048(4) Å) < 4,4′-Br$_2$-2,2′-

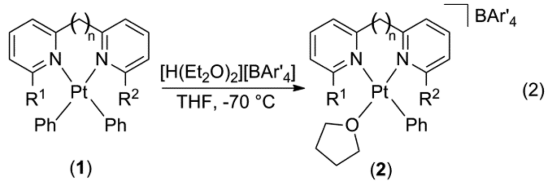

(2)

n = 1, R^1 = H, R^2 = Me (**1b**, **2b**), 93% isolated yield
n = 1, R^1 = R^2 = Me (**1c**, **2c**), 95% isolated yield
n = 0, R^1 = R^2 = Me (**1d**, **2d**), 91% isolated yield
n = 2, R^1 = R^2 = H (**1e**, **2e**), 89% isolated yield

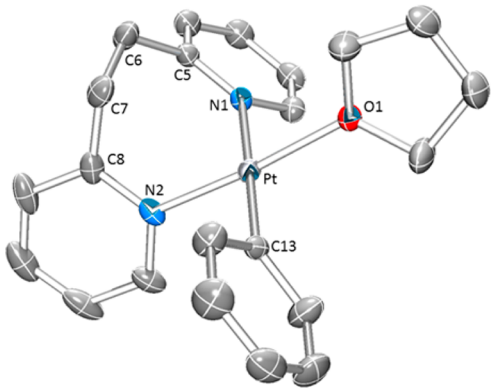

Figure 2. ORTEP drawing of [(dpe)Pt(Ph)(THF)][BAr′$_4$] (**2e**) (50% probability; BAr′$_4$ anion and H atoms omitted for clarity). Selected bond lengths (Å): Pt–N1 = 2.141(4), Pt–N2 = 1.980(4), Pt–O1 = 2.048(4), Pt–C13 = 2.001(5). Selected bond angles (deg): N1–Pt–N2 = 87.9(2), O1–Pt–C13 = 93.2(2).

dx.doi.org/10.1021/om400390e | *Organometallics* 2013, 32, 3903–3913

Table 2. Comparison of Catalytic Ethylene Hydrophenylation Using Complexes 2a−e[a]

Entry	Complex				*o:m:p*[b]	TOF[c] (10^{-3} s^{-1})	% Diethylbenzene[d]
1	**2a**	55.3[e] (194.9)[f] [370.9][g]	0.4 (1.1) [2.3]	10.6 (39.2) [95.9]	1:9.8:6.8	5.1	20.4
2	**2b**	31.2 (54.1) [57.9]	2.7 (4.2) [4.9]	1.3 (2.3) [2.3]	1:0.8:0.8	5.1	3.5
3	**2c**	19.5 (22.3) [26.6]	1.7 (1.9) [2.3]	trace (0.3) [0.5]	1:0:0	4.6	1.7
4	**2d**	0 (0) [0]	0.7 (0.7) [0.7]	0 (0) [0]	-	-	0
5	**2e**	0.7 (0.8) [0.8]	0.4 (0.4) [0.4]	0 (0) [0]	-	-	0

[a]Conditions: 0.01 mol % of catalyst dissolved in C_6H_6 with hexamethylbenzene as an internal standard at 100 °C with 0.1 MPa of C_2H_4. [b]Ratio of 1,2-, 1,3-, and 1,4-diethylbenzene after 4 h. [c]Turnover frequency calculated after 1 h. [d]Percent of diethylbenzenes in the total arene product after catalyst deactivation. [e]Turnovers after 4 h as determined by GC/MS. [f]Numbers in parentheses are turnovers after 16 h. [g]Numbers in brackets are TON.

bipyridine (2.060(7) Å) < cyclooctadiene (2.077(2) Å) < $[Ph_2B(CH_2PPh_2)_2]^-$ (2.170(4) Å).

Ethylene hydrophenylation was evaluated using **2b−e** as catalyst precursors, and the results are summarized in Table 2. The catalyst data for the previously reported dipyridylmethane-ligated Pt^{II} complex $[(dpm)Pt(Ph)(THF)][BAr'_4]$ (**2a**) are included for comparative purposes.[9c] Using data after 4 h at 100 °C under 0.1 MPa of ethylene, complex **2a** is the most effective catalyst with 65.9 turnovers (TO) of ethylbenzenes (the formation of diethylbenzene is counted as one TO) and trace styrene. Using **2a**, an ultimate turnover number (TON) of 469 is achieved after approximately 4 days. The incorporation of methyl substituents in the 6/6′-positions of dpm or 2,2′-bipyridine ligands (**2b−d**) or an increase in the chelate ring size from a six-membered to a seven-membered ring using 1,2-bis(2-pyridyl)ethane (**2e**) results in a decrease in overall catalyst efficiency relative to **2a** (see Table 2 and Figure 3).

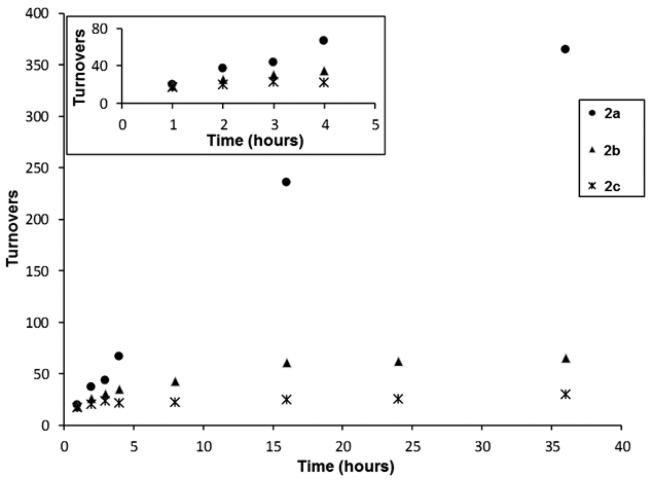

Figure 3. Plot of TO versus time for ethylene hydrophenylation (100 °C) catalyzed by complexes **2a−c** using 0.01 mol % of catalyst dissolved in C_6H_6 with 0.1 MPa of C_2H_4 and hexamethylbenzene as an internal standard. The inset highlights turnovers as function of time for the first 4 h of catalysis.

The asymmetric complex **2b**, with a methyl group in the 6-position of one pyridyl ring, provides 35.2 TO of ethylbenzenes and styrene after 4 h. The orientation of the phenyl ligand and methyl substituent on the bpy ligand of complex **2b** has not been determined. The inclusion of methyl groups into both 6-positions of the dipyridyl ligand (complex **2c**) results in a total of 21.2 TO of ethylbenzene and styrene after 4 h. Thus, among complexes **2a−c** using data after 4 h of reaction, the addition of each methyl group reduces the catalytic turnover by ∼40%. Furthermore, the presence of 6/6′-substituents results in a change in ethylbenzene to styrene ratios. For example, after 4 h, complex **2a** produces ethylbenzene and styrene in an approximate 138:1 ratio, in comparison to ∼11:1 for both **2b** and **2c**. For catalysis using $[(^tbpy)Pt(Ph)(THF)][BAr'_4]$, computational studies are consistent with β-hydride elimination following ethylene insertion into the Pt−Ph bond to form $[(^tbpy)Pt(H)(\eta^2\text{-}CH_2CHPh)]^+$ being rapid and reversible.[9b] The increased sterics around the Pt center provided by the methyl substituents of **2b,c** might facilitate styrene displacement and have the effect of decreasing the ethylbenzene/styrene ratio. Also, if the formation of unstable Pt^{II}−hydride complexes provides the primary pathway for catalyst decomposition,[9b] facilitating styrene dissociation would be expected to decrease the TON, which is consistent with the data shown in entries 1−3 in Table 2.

Figure 3 shows TO versus time for the hydrophenylation of ethylene using catalysts **2a−c**. Unlike **2a**, complexes **2b,c** exhibit signs of decomposition in less than 4 h at 100 °C with 0.01 mol % of Pt catalyst. In order to mitigate the influence of catalyst decomposition and offer a direct comparison between the complexes, turnover frequencies (TOF) were evaluated early in the reaction. After 1 h at 100 °C, complex **2a** catalyzes the formation of 18.6 TO of ethylbenzenes and styrene for a TOF of 5.1×10^{-3} s^{-1}. Complexes **2b,c** perform similarly with 18.2 (TOF = 5.1×10^{-3} s^{-1}) and 16.5 TO (TOF = 4.6×10^{-3} s^{-1}), respectively. Thus, the decreased catalytic TON observed with increasing 6/6′-substitution of the dpm ligand is a likely result of increased rates of catalyst decomposition as opposed to decreased catalytic activity. We have modeled the rate of catalyst decomposition using first-order and second-order plots

dx.doi.org/10.1021/om400390e | *Organometallics* 2013, 32, 3903−3913

of TOF as a function of time (see the Supporting Information for details). Excellent fits ($R^2 \geq 0.98$) were obtained for complexes **2a**–**c** using second-order plots (Figure 4). The

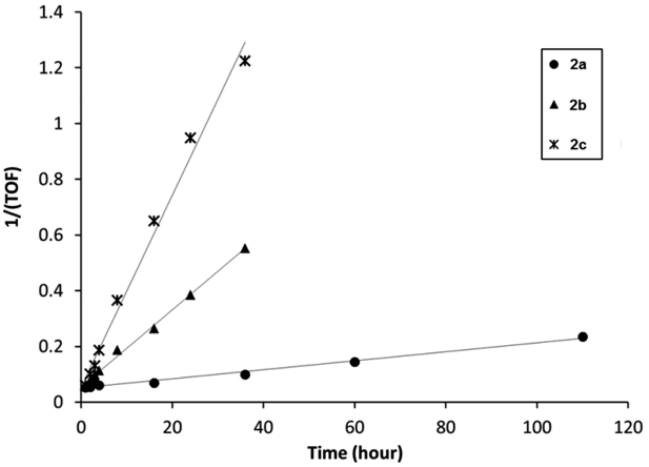

Figure 4. Plot of 1/TOF versus time demonstrating the second-order decomposition of complexes **2a**–**c** ($R^2 \geq 0.98$ for all three fits).

kinetic analysis of catalyst decomposition reveals that the second-order rate constant for decomposition of complex **2a** is $1.61(8) \times 10^{-3}$ s^{-1} M^{-1}. In comparison, the rate of decomposition of the monomethyl complex **2b** is close to 1 order of magnitude larger ($1.38(3) \times 10^{-2}$ s^{-1} M^{-1}), and the rate of decomposition for the dimethyl complex **2c** is accelerated by a factor of ~2.5 ($3.4(1) \times 10^{-2}$ s^{-1} M^{-1}) relative to **2b**.

Using [(Me_2-bpy)Pt(Ph)(THF)][BAr'_4] (**2d**) as a catalyst precursor for ethylene hydrophenylation results in styrene production with 0.7 TO (relative to **2c**) along with small quantities of (vinyl)ethylbenzene isomers, which were not quantified. No evidence for the formation of ethylbenzenes was obtained. The selectivity for vinylarene production is in contrast to that for a previously reported unsubstituted bipyridine ligated Pt^{II} precursor for ethylene hydrophenylation.[17] The reaction of **2d** with ethylene at room temperature in CD_2Cl_2 readily produces styrene quantitatively with the formation of multiple intractable Pt complexes, as observed by ^1H NMR spectroscopy (eq 3). The putative intermediate

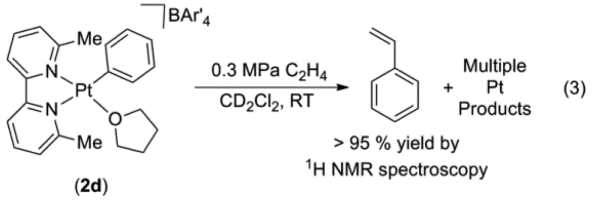

(3)

[(Me_2-bpy)Pt(CH_2CH_2Ph)]$^+$ likely undergoes rapid β-hydride elimination and net dissociation of styrene, with the resulting Pt–H complex [(Me_2-bpy)Pt(H)]$^+$ decomposing rapidly. Expansion to a seven-membered chelate using [(dpe)Pt(Ph)-(THF)][BAr'_4] (**2e**) results in 1.2 TO of ethylbenzene and styrene in an approximate 2:1 ratio upon heating in benzene with 0.1 MPa of ethylene. Decreasing the temperature to 80 °C for complex **2e** did not extend catalyst longevity, as only 1.5 total TO of ethylbenzene and styrene were observed. Rapid decomposition of the catalyst is likely due to the poor stability of seven-membered chelates (in comparison to their five- or six-membered counterparts)[18] or facile displacement of 1,2-bis(pyridyl)ethane from transient Pt^{IV} intermediates.[15]

One issue with ethylene hydrophenylation catalyzed by formally cationic bipyridyl Pt^{II} complexes is the formation of diethylbenzenes.[8b,9b–d] For example, diethylbenzenes constitute approximately 20% of the total alkyl arene product from ethylene hydrophenylation with **2a** and [(^{t}bpy)Pt(Ph)(THF)]-[BAr'_4] (**^{t}bpyPt**). This result has been attributed to competition between ethylbenzene C–H activation and net dissociation of ethylbenzene from the metal center.[9b] While the percent composition of diethylbenzenes from catalysis using **2a** is not improved relative to catalysis using **^{t}bpyPt**, the regioselectivity of diethylbenzene formation is influenced. For complex **2a**, the ratio of meta/para to ortho diethylbenzenes is ~17:1 at 100 °C, which is 4 times greater than that reported for **^{t}bpyPt** (eq 4). Introducing steric perturbations in the 6/6′-

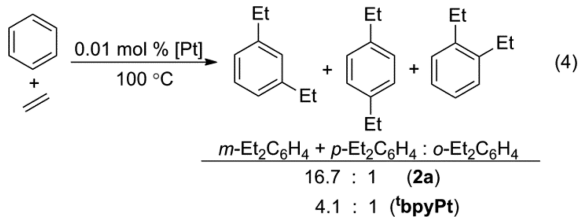

(4)

positions of the dipyridylmethane ligand influences the selectivity for monoalkylation versus dialkylation of benzene. Analysis of the reaction mixture from a reaction of benzene and ethylene after 16 h using complex **2b** yields a total of 60.6 TO, of which only ~4% are diethylbenzenes, similar to the observation with a reported formally neutral Pt^{II} catalyst precursor.[8c] With complex **2c**, diethylbenzenes represent <2% of the total arene product after complete catalyst deactivation, and catalysis with complexes **2d**,**e** results in no observable diethylbenzene formation. Therefore, while methyl groups in the 6-positions of the pyridyl rings decrease catalytic TO, the formation of diethylbenzenes is suppressed.

Ethylene hydroarylation using ethylbenzene as the aromatic substrate was probed (Table 3). Using data after 4 h of reaction, the observed catalytic activity was significantly reduced in comparison to hydroarylation of ethylene using benzene for complexes **2a**–**e**. Note that this comparison

Table 3. Comparison of Catalytic Ethylene Hydroarylation with Ethylbenzene Using Complexes 2a–e[a]

Complex			
2a	5.6[b] (13.6)[c]	4.1 (9.4)	0 (trace)
2b	2.1 (6.5)	1.1 (3.0)	0 (trace)
2c	0.8 (1.9)	0.5 (1.0)	0.5 (1.0)
2d	0 (0)	0 (0)	0 (0)
2e	0 (trace)	0 (0)	0 (0)

[a]Conditions: 0.01 mol % of catalyst dissolved in C_6H_6 with hexamethylbenzene as an internal standard at 100 °C with 0.1 MPa of C_2H_4. [b]Turnovers after 4 h as determined by GC/MS. [c]Numbers in parentheses are turnovers after 16 h.

dx.doi.org/10.1021/om400390e | Organometallics 2013, 32, 3903–3913

assumes negligible catalyst deactivation after 4 h (see above). Thus, the observed relative rates of ethylene hydroarylation using benzene and ethylbenzene are opposite to those of catalysis using a Friedel–Crafts catalyst.[19] For the Pt^{II} catalysts, the decreased hydroarylation activity using ethylbenzene as the aromatic substrate and the low concentration of ethylbenzene during ethylene hydro*phenylation* (due to a low catalyst loading) strongly suggest that the formation of diethylbenzenes from the reaction of benzene with ethylene does not originate from the catalyst reacting with free ethylbenzene generated in situ.

Complex **2a** catalyzes the formation of 9.7 and 23.0 TO of diethylbenzenes after 4 and 16 h, respectively. The ratio of meta to para substitution was ~1.4:1, and the formation of 1,2-diethylbenzene was observed only in trace amounts. Using complex **2b**, the meta to para ratio is nearly identical with that observed for **2a** and the formation of 1,2-diethylbenzene was not observed in quantifiable amounts. Catalysis with **2c** exhibits little selectivity, as the formation of 1,2-diethylbenzene is equal to the formation of 1,4-diethylbenzene. No quantifiable amounts of diethylbenzenes were detected with complexes **2d,e** over a period of 16 h from the reaction with ethylene and ethylbenzene.

Catalytic olefin hydroarylation using substituted olefins and a nonacidic pathway offers an opportunity to control the selectivity for Markovnikov/anti-Markovnikov products. For example, catalysts that can bias 2,1- over 1,2-insertion with α-olefins could selectively produce linear alkyl arenes, which are not accessible with current acid-based methodologies. Propylene hydrophenylation with **^{t}bpyPt** results in the formation of both cumene and *n*-propylbenzene in an approximate 3:1 ratio.[8b] Catalysis using propylene with complexes **2a–e** was performed to determine the influence of steric modifications on regioselectivity (Table 4). At 100 °C under 0.1 MPa of propylene, cumene (9.6 TO) and *n*-propylbenzene (2.2) are produced in a 4.4:1 ratio after 4 h with complex **2a**. The ratio of branched to linear products is almost invariant with time. Thus, the six-membered chelate of **2a** increases the branched to linear ratio by ~50% in comparison to that observed for the bipyridyl-supported catalyst.[8b] The sequential addition of methyl groups to the 6-positions of the pyridyl rings of dipyridylmethane heightens the propensity for cumene formation over *n*-propylbenzene. Using complex **2b**, a ratio of branched to linear isomers of 5.3 is observed after 4 h of catalysis. The symmetrically substituted Me_2-dpm complex **2c** is completely selective for the formation of cumene in substoichiometric amounts. The formation of several isomers of (propenyl)-propylbenzene was detected by GC/MS but not quantified. As observed during catalysis with ethylene, complex **2d** readily undergoes β-hydride elimination following propylene insertion into the Pt–Ph bond, and only 2-phenylpropylene is observed after 16 h but was not quantified. Complex **2e** is selective for the formation of cumene in ~40% yield, relative to **2e.** Whether the cumene to *n*-propylbenzene ratios are controlled by the regioselectivity of propylene insertion or by the relative rates of subsequent reactions (i.e., Curtin–Hammett conditions) is not known; thus, rationalizing any trend is difficult.

The substitution of ^{t}bpy with dpm provides enhanced activity and longevity for Pt^{II}-catalyzed ethylene hydrophenylation.[9c] We sought to determine the influence of the dipyridyl linkage identity on catalytic activity and selectivity. A series of catalyst precursors were synthesized in which the methylene bridge between pyridyl rings of dpm was substituted with C=O (**4a**), NH (**4b**), and O (**4c**) following the procedure for complexes **2** (eq 5). Under conditions of 100 °C and 0.1 MPa of ethylene,

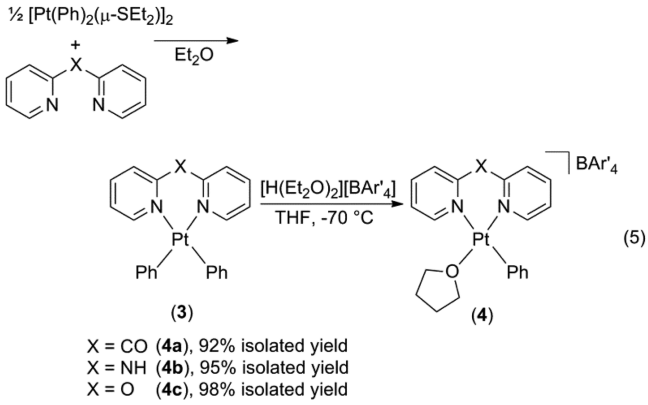

(5)

the catalytic activities of complexes **4a–c** were evaluated (Table 5). Comparison of the TO observed after 4 h demonstrates that catalytic efficiency decreases in the following order: CH_2 (**2a**) > NH (**4b**) > CO (**4a**) > O (**4c**). Note that catalyst

Table 4. Comparison of Catalytic Propylene Hydrophenylation Using Complexes 2a–e and ^{t}bpyPt[a]

Complex	^{i}Pr	^{n}Pr	B:L[b]
^{t}bpyPt[e]	25.0[c] 29.7[d]	8.5 10.1	2.9
2a	9.6 (20.9)	2.2 (5.1)	4.4
2b	2.1 (3.8)	0.4 (0.9)	5.3
2c	0.6 (0.7)	0 (0)	-
2d[f]	0 (0)	0 (0)	-
2e	0.3 (0.4)	0 (0)	-

[a]Conditions: 0.01 mol % of catalyst dissolved in C_6H_6 with hexamethylbenzene as an internal standard at 100 °C with 0.1 MPa of C_3H_6. [b]Ratio of cumene to *n*-propylbenzene after 4 h. [c]Turnovers after 4 h as determined by GC/MS. [d]Numbers in parentheses are turnovers after 16 h. [e]Catalysis data from ref 8b. [f]Minor production of 2-phenylpropylene observed.

Table 5. Comparison of Catalytic Ethylene Hydrophenylation Using Complexes 4a–c[a]

Complex	Et		Et, Et	*o:m:p*[b]
2a	55.3[c] (194.9)[d]	0.4 (1.1)	10.6 (39.2)	1:9.8:6.8
4a	3.3 (3.6)	1.9 (2.1)	0 (0)	-
4b	18.6 (25.4)	2.5 (3.4)	4.0 (5.5)	5.6:3.5:1
4c	1.6 (3.1)	2.9 (4.6)	0 (0)	-

[a]Conditions: 0.01 mol % of catalyst dissolved in C_6H_6 with hexamethylbenzene as an internal standard at 100 °C with 0.1 MPa of C_2H_4. [b]Ratio of 1,2-, 1,3-, and 1,4-diethylbenzene after 4 h. [c]Turnovers after 4 h as determined by GC/MS. [d]Numbers in parentheses are turnovers after 16 h.

dx.doi.org/10.1021/om400390e | *Organometallics* 2013, 32, 3903–3913

decomposition complicates any comparison of activity using these data. The dipyridylamine complex [(dpa)Pt(Ph)(THF)][BAr′$_4$] (**4b**; dpa = bis(2-pyridyl)amine) provides a total of 25.1 TO after 4 h, which is more than a 60% decrease in TO compared to the case for **2a**. Catalysis with [(dpk)Pt(Ph)(THF)][BAr′$_4$] (**4a**; dpk = bis(2-pyridyl)ketone) results in only 3.3 and 1.9 TO of ethylbenzene and styrene, respectively, after 4 h. Using dipyridyl ether in [(dpo)Pt(Ph)(THF)][BAr′$_4$] (**4c**; dpo = bis(2-pyridyl) ether) provides a total of 4.5 TO after 4 h, favoring styrene production. In all cases, substitution of the methylene linkage reduces catalyst TO and longevity; the latter is evident by the marginal changes in TO after 16 h in comparison to the TO after 4 h for catalysis using **4a−c**. Diethylbenzenes were only observed during catalysis with **4b** and constitute ∼16% of the total arene products. As previously observed with bipyridyl donor variations,[9d] changing the identity of the pyridyl linkage has an influence on styrene production. As the linkage becomes more electron withdrawing, the ratio of ethylbenzene to styrene decreases. For example, the amine linkage in complex **4b** produces ethylbenzene and styrene in a 7.4:1 ratio, which is a 95% decrease in comparison to that for the parent dpm ligand. The ratio further decreases for carbonyl and ether linkages with observed ratios of 1.7:1 and 0.6:1 for complexes **4a**,**c**, respectively.

The results of catalysis employing ethylbenzene as the aromatic substrate for complexes **4a−c** are similar to those observed for complexes **2** (Table 6). For all complexes, 1,2-diethylbenzene was not detected after 16 h. Complex **4a** produces approximately equimolar amounts of 1,3- and 1,4-diethylbenzene with complete cessation of catalytic activity after 4 h. Meta- and para-substituted diethylbenzenes are also observed in an approximate 1:1 ratio using complex **4b** after 4 h with a total of 4.3 TO after 16 h, slightly favoring meta substitution. Complex **4c** yields substoichiometric amounts of diethylbenzenes for an approximate 50% yield after 16 h.

Table 6. Comparison of Catalytic Ethylene Hydroarylation with Ethylbenzene Using Complexes 4a−c[a]

Complex			
4a	0.9[b] (1.1)[c]	0.7 (0.9)	0 (0)
4b	0.7 (2.5)	0.6 (1.8)	0 (0)
4c	trace (0.2)	trace (0.3)	0 (0)

[a]Conditions: 0.01 mol % of catalyst dissolved in C_6H_6 with hexamethylbenzene as an internal standard at 100 °C with 0.1 MPa of C_2H_4. [b]Turnovers after 4 h as determined by GC/MS. [c]Numbers in parentheses are turnovers after 16 h.

Catalysis using propylene and benzene with complexes **4a−c** was then studied to probe the influence of pyridyl linker on selectivity (Table 7). For **4a−c**, the regioselectivity is biased toward cumene, and the ratio of Markovnikov to anti-Markovnikov addition products increases slightly for **4a−c** in comparison to **2a**. At 100 °C under 0.1 MPa of propylene, complex **4b** was found to be the most active catalyst precursor for propylene hydrophenylation with 25.4 TO of cumene and *n*-propylbenzene in a 5.2:1 ratio after 4 h. Using complex **4a**, only 5.0 TO are observed after 4 h with a branched to linear ratio of 6.1:1, and extended reaction times result in no further catalytic activity. Propylene hydrophenylation with the dipyridyl ether complex **4c** after 4 h results in a product distribution nearly identical with that of **4a** with 4.9 TO of cumene and *n*-propylbenzene in a 7.2:1 ratio. As the TO values of cumene are the same for **4a** and **4c** and the TO value of *n*-propylbenzene differs by only 0.1, the regioselectivity of insertion into the Pt−Ph bond is approximately the same for these complexes.

Table 7. Comparison of Catalytic Propylene Hydrophenylation Using Complexes 4a−c[a]

Complex			B:L[b]
4a	4.3[c] (4.4)[d]	0.7 (0.7)	6.1
4b	21.3 (27.9)	4.1 (5.5)	5.2
4c	4.3 (4.9)	0.6 (0.7)	7.2

[a]Conditions: 0.01 mol % of catalyst dissolved in C_6H_6 with hexamethylbenzene as an internal standard at 100 °C with 0.1 MPa of C_3H_6. [b]Ratio of cumene and *n*-propylbenzene after 4 h. [c]Turnovers after 4 h as determined by GC/MS. [d]Numbers in parentheses are turnovers after 16 h.

CONCLUSION

We have studied the systematic variation of ligand steric and electronic properties for dipyridyl Pt^{II} catalyzed olefin hydroarylation. Modifications include substitution at the 6,6′-position(s) of the pyridyl rings with methyl groups, expansion to a seven-membered chelate ring with 1,2-(dipyridyl)ethane, and changes in the identity of the functionality that bridges pyridyl rings. In comparison to the parent dipyridylmethane-ligated Pt^{II} catalyst precursor, introducing steric modification proximal to the metal center with methyl groups in the 6/6′-positions of the pyridyl rings increases selectivity for monosubstituted benzenes with catalytic activity similar to that of the dpm complex **2a** for ethylene hydrophenylation; however, the rate of catalyst decomposition is accelerated. If conditions to stabilize similar catalysts can be developed, these sterically bulky ligands are promising targets for both active and selective ethylbenzene synthesis. The ratios of ethylbenzene to styrene decrease with substitution at the 6,6′-positions likely due to facilitation of styrene displacement. 2,2′-Bipyridyl-ligated Pt^{II} precursors featuring 6/6′-substitution are catalytically inactive, as β-hydride elimination is preferred over aromatic C−H activation. Replacing the methylene bridge with carbonyl, amine, or ether groups also results in decreased catalytic activity for ethylene hydrophenylation. All the complexes discussed herein have significantly reduced catalytic efficiency for ethylene hydroarylation using ethylbenzene, which is in contrast with acid-catalyzed pathways. The formation of Markovnikov addition products using propylene is favored with increasing steric congestion around the metal center and an electron-withdrawing pyridyl bridge functionality.

In terms of future olefin hydroarylation catalyst design, the following conclusions are pertinent: the key to long-lived catalytic production of alkyl arenes appears to be avoiding vinylarene formation. If vinylarene production is desired, a sterically crowded 2,2′-bipyridyl ligand is preferred, such as **2d**. For efficient styrene production, the issue of catalyst decomposition will need to be overcome, which is possibly

dx.doi.org/10.1021/om400390e | *Organometallics* 2013, 32, 3903−3913

due to the formation of unstable Pt−H intermediates that result from β-hydride elimination and styrene dissociation. Thus, it is clear that square-planar Pt^{II} complexes provide a sterically and electronically flexible catalyst platform by which both activity and selectivity for the synthesis of $C_{aryl}-C_{sp^3}$ linkages, important in both bulk and fine chemical synthesis, may be produced directly from hydrocarbon starting materials without the need for intermediate functionalization steps.

EXPERIMENTAL SECTION

General Methods. Unless otherwise noted, all synthetic procedures were performed under anaerobic conditions in a nitrogen-filled glovebox or by using standard Schlenk techniques. Glovebox purity was maintained by periodic nitrogen purges and was monitored by an oxygen analyzer (O_2 <15 ppm for all reactions). Acetonitrile and diethyl ether were dried by distillation over CaH_2. Tetrahydrofuran and *n*-pentane were distilled over sodium/benzophenone and P_2O_5, respectively. Methylene chloride and benzene were purified by passage through a column of activated alumina. Benzene-d_6, acetone-d_6, and dichloromethane-d_2 were used as received and stored under a N_2 atmosphere over 4 Å molecular sieves. ^{1}H NMR spectra were recorded on a Varian Mercury 300 MHz, Unity Avance 500 MHz, Bruker 400 MHz, or Bruker 800 MHz spectrometer. ^{13}C NMR spectra were recorded using a Varian Mercury 300 MHz (operating frequency 75 MHz), Unity Avance 500 MHz (operating frequency 125 MHz), or Bruker 800 MHz (operating frequency 201 MHz) spectrometer. All ^{1}H and ^{13}C NMR spectra are referenced against residual proton signals (^{1}H NMR) or the ^{13}C resonances (^{13}C NMR) of the deuterated solvents. ^{19}F NMR (282 MHz operating frequency) spectra were obtained on a Varian 300 MHz spectrometer and referenced against an external standard of hexafluorobenzene (δ −164.9 ppm). GC/MS was performed using a Shimadzu GCMS-QP2010 Plus system with a 30 m × 0.25 mm SHRXI-5MS column with 0.25 mm film thickness using negative chemical ionization (NCI), which also allows for simulated electron impact (SEI) ionization. Microwave synthesis was performed using a Biotage Initiator EXP, in addition to caps and vials purchased from Biotage. The mass spectral data were obtained from a Bruker 9.4 T Apex-Qe Hybrid Qe-Fourier Transform Ion Cyclotron Resonance (FT-ICR) mass spectrometer equipped with an Apollo II electrospray ionization source. The sample was reconstituted with 200 μL of acetonitrile, and a 3.5 μL aliquot was diluted with 50 μL of 60% acetonitrile/0.1% formic acid prior to directly infusing into the FT-ICR MS via a TriVersa NanoMate (Advion BioScience). Exact masses were obtained for the entire broadband spectrum. Instrument parameters were adjusted to maximize the signals around the peak of interest. Bruker Daltonics DataAnalysis software (v.3.4) was utilized for the analysis of the data, and assignments were made on the basis of exact mass measurements and fit of isotopic peaks to theoretical isotopic patterns (IsotopePattern algorithm, Bruker). Errors between observed and theoretical peaks are reported in ppm. Elemental analysis was performed by Atlantic Microlabs, Inc. Ethylene (99.5%) and propylene (99.5%) were purchased in a gas cylinder from GTS-Welco and used as received. All other reagents were used as purchased from commercial sources. The preparation, isolation, and characterization of $[H(Et_2O)_2][BAr'_4]$ (Ar′ = 3,5-$(CF_3)_{2b6}H_3$),[20] $[Pt(Ph)_2(Et_2S)]_2$,[21] 6-methyl-2,2′-dipyridylmethane,[22] 6,6′-dimethyl-2,2′-dipyridylmethane,[22] 1,2-bis(2-pyridyl)ethane,[23] (dpm)Pt$(Ph)_2$ (**1a**),[9c] [(dpm)Pt(Ph)(THF)][BAr′$_4$] (**2a**),[9c] and [(^{t}bpy)Pt(Ph)(THF)][BAr′$_4$] (**^{t}bpyPt**)[9b] have been previously reported.

Synthesis of Bis(2-pyridyl) Ether (dpo). A method for synthesizing bis(2-pyridyl) ether was developed from previous protocols[24] using convenient starting materials. Microwave-assisted synthesis in sealed vials reduces reaction times and increases the yield of desired product over that of prior work without resorting to high-boiling solvents such as DMF. In an oven-dried microwave vial with a magnetic stir bar, 2-bromopyridine (1.0 g, 6.3 mmol), 2-hydroxypyridine (0.90 g, 9.5 mmol), cesium carbonate (6.2 g, 19 mmol), and dry acetonitrile (15 mL) were added under a flow of nitrogen. The vial was sealed and subjected to microwave heating (Initiator EXP, Biotage) at 200 °C with a maximum pressure of 1.8 MPa for 1 h. The solid was removed by filtration and washed with acetonitrile. The deep orange filtrate was then dried by rotary evaporation to give a thick oily residue. Purification by column chromatography on silica gel with 3:2 ethyl acetate:hexanes afforded the product as an oil which solidifies at room temperature. Isolated yield: 0.56 g (51%). ^{1}H NMR (400 MHz, $CDCl_3$): δ 8.29 (ddd, $^3J_{HH}$ = 5 Hz, $^4J_{HH}$ = 2 Hz, $^5J_{HH}$ = 1 Hz, 2H, 6-dpo), 7.76 (ddd, $^3J_{HH}$ = 8 Hz, $^3J_{HH}$ = 7 Hz, $^4J_{HH}$ = 2 Hz, 2H, 4-dpo), 7.09 (m, 4H, 3- and 5-dpo). ^{13}C NMR (125 MHz, $CDCl_3$): δ 162.3, 148.5, 139.9, 120.3, 114.4. ESI-FTICR MS: calcd for $[C_{10}H_9N_2O]^+$ 173.0709, found 173.0707. Anal. Calcd for $C_{10}H_8N_2O$: C, 69.76; H, 4.68; N, 16.27. Found: C, 69.55; H, 4.77; N, 16.32.

General Procedure for the Synthesis of (N∼N)PtPh$_2$ Complexes (1b−e and 3a−c). To a suspension of $[Pt(Ph)_2(Et_2S)]_2$ in Et_2O (30 mL), was added 2 equiv of the appropriate ligand. The solution was stirred at room temperature for approximately 12 h. The solution was reduced in vacuo, and hexanes were added (∼20 mL). The solution was filtered, and the precipitate was washed with Et_2O (1 × 5 mL) and hexanes (2 × 5 mL) and dried under vacuum.

*(Me-dpm)PtPh$_2$ (**1b**).* The ligand was 6-methyl-2,2′-dipyridylmethane (Me-dpm). Isolated yield: 0.19 g (92%). ^{1}H NMR (800 MHz, CD_2Cl_2): δ 8.54 (ddd, $^3J_{HH}$ = 6 Hz, $^4J_{HH}$ = 2, $^5J_{HH}$ = 1 Hz, 1H, 6-dpm), 7.72 (td, $^3J_{HH}$ = 8 Hz, $^4J_{HH}$ = 2 Hz, 1H, 4-dpm), 7.64 (t, $^3J_{HH}$ = 8 Hz, 1H, 4-dpm), 7.51 (dd, $^3J_{HH}$ = 8 Hz, $^4J_{HH}$ = 1 Hz, 2H, H^o-Ph), 7.46 (d, $^3J_{HH}$ = 7 Hz, 1H, 3-dpm), 7.37 (d, $^3J_{HH}$ =8 Hz, 1H, 3-dpm), 7.19 (dd, $^3J_{HH}$ = 8 Hz, $^4J_{HH}$ = 1 Hz, 1H, H^o-Ph), 7.09 (ddd, $^3J_{HH}$ = 7 Hz, $^3J_{HH}$ = 6 Hz, $^4J_{HH}$ = 1 Hz, 1H, 5-dpm), 7.05 (d, $^3J_{HH}$ = 7 Hz, 1H, 5-dpm), 6.88 (t, $^3J_{HH}$ = 8 Hz, 2H, H^m-Ph), 6.77−6.72 (m, 3H, H^m- and H^p-Ph), 6.68 (tt, $^3J_{HH}$ = 8 Hz, $^4J_{HH}$ = 1 Hz, 1H, H^p-Ph), 5.67 (d, $^2J_{HH}$ = 14 Hz, 1H, dpm-CH_2), 4.26 (d, $^2J_{HH}$ = 14 Hz, 1H, dpm-CH_2), 2.38 (s, 3H, dpm-Me). ^{13}C NMR (201 MHz, CD_2Cl_2): δ 162.7, 156.3, 156.1, 151.1, 146.2, 141.0, 138.5, 138.4, 137.9, 137.8, 126.9, 126.2, 124.9, 124.7, 123.8, 121.9, 121.5, 121.5 (Me-dpm and Ph aromatic), 47.7 (dpm-CH_2), 26.7 (dpm-Me). Anal. Calcd for $PtN_2C_{24}H_{22}$: C, 54.02; H, 4.16; N, 5.25. Found: C, 54.06; H, 4.28; N, 5.21.

*(Me$_2$-dpm)PtPh$_2$ (**1c**).* The ligand was 6,6′-dimethyl-2,2′-dipyridylmethane (Me$_2$-dpm). Isolated yield: 0.32 g (94%). ^{1}H NMR (800 MHz, acetone-d_6): δ 7.75 (t, $^3J_{HH}$ = 8 Hz, 2H, 4-dpm), 7.60 (d, $^3J_{HH}$ = 8 Hz, 2H, 3-dpm), 7.37 (dd, $^3J_{HH}$ = 8 Hz, $^4J_{HH}$ =1 Hz, 4H, H^o-Ph), 7.15 (d, $^3J_{HH}$ = 8 Hz, 1H, 5-dpm), 6.68 (t, $^3J_{HH}$ = 8 Hz, 4H, H^m-Ph), 6.57 (t, $^3J_{HH}$ = 8 Hz, 2H, H^p-Ph), 6.11 (d, $^2J_{HH}$ = 14 Hz, 1H, dpm-CH_2), 4.69 (d, $^2J_{HH}$ = 14 Hz, 1H, dpm-CH_2), 2.53 (s, 6H, dpm-Me). ^{13}C NMR (201 MHz, acetone-d_6): δ 162.4, 157.3, 141.6, 139.1, 138.8, 126.4, 124.9, 122.7, 121.4 (dpm and Ph aromatic), 47.5 (dpm-CH_2), 26.1 (dpm-Me). Anal. Calcd for $PtN_2C_{25}H_{24}$: C, 54.83; H, 4.43; N, 5.12. Found: C, 54.33; H, 4.30; N, 5.11.

*(Me$_2$-bpy)PtPh$_2$ (**1d**).* The ligand was 6,6′-dimethyl-2,2′-bipyridine (Me$_2$-bpy). Isolated yield: 0.230 g (69%). ^{1}H NMR (800 MHz, acetone-d_6): δ 8.38 (d, $^3J_{HH}$ = 8 Hz, 2H, bpy), 8.16 (t, $^3J_{HH}$ = 8 Hz, 2H, bpy), 7.48 (d, $^3J_{HH}$ = 7 Hz, 2H, bpy), 7.40 (d, $^3J_{HH}$ = 7 Hz, 4H, H^o-Ph), 6.80 (t, $^3J_{HH}$ = 7 Hz, 4H, H^m-Ph), 6.69 (t, $^3J_{HH}$ = 7 Hz, 2H, H^p-Ph). ^{13}C NMR (201 MHz, acetone-d_6): δ 163.3, 157.8, 142.8, 139.4, 139.0, 127.5, 126.8, 121.6, 120.3 (bpy and Ph aromatic), 26.7 (CH_3-bpy). Anal. Calcd for $PtN_2C_{24}H_{22}$: C, 54.02; H, 4.16; N, 5.25. Found: C, 54.26; H, 4.32; N, 5.17.

*(dpe)PtPh$_2$ (**1e**).* The ligand was 1,2-bis(2-pyridyl)ethane (dpe). Isolated yield: 0.19 g (76%). ^{1}H NMR (500 MHz, CD_2Cl_2): δ 8.71 (dd, $^3J_{HH}$ = 6 Hz, $^4J_{HH}$ = 2 Hz, 2H, 6-dpe), 7.57 (td, $^3J_{HH}$ = 8 Hz, $^4J_{HH}$ = 2 Hz, 2H, 4-dpe), 7.45 (dd, $^3J_{HH}$ = 8 Hz, $^3J_{HH}$ = 1 Hz, $^3J_{PtH}$ = 72 Hz Pt satellites, 4H, H^o-Ph), 7.23 (d, $^3J_{HH}$ = 8 Hz, 2H, 3-dpe), 6.99 (ddd, $^3J_{HH}$ = 8 Hz, $^3J_{HH}$ = 6 Hz, $^4J_{HH}$ = 1 Hz, 2H, 5-dpe), 6.82 (t, $^3J_{HH}$ = 7 Hz, 4H, H^m-Ph), 6.71 (t, $^3J_{HH}$ = 7 Hz, 2H, H^p-Ph), 4.21 (br s, 4H, dpe-CH_2). ^{13}C NMR (125 MHz, CD_2Cl_2): δ 160.40, 151.52, 143.01, 138.81, 137.30, 126.57, 126.35, 122.99, 121.60 (dpe and Ph aromatic), 34.83 (dpe-CH_2). Anal. Calcd for $PtN_2C_{24}H_{22}$: C, 54.02; H, 4.16; N, 5.25. Found: C, 53.98; H, 4.13; N, 5.17.

*(dpk)PtPh$_2$ (**3a**).* The ligand was bis(2-pyridyl)ketone (dpk). Isolated yield: 0.21 g (91%). ^{1}H NMR (300 MHz, acetone-d_6): δ 8.49 (ddd, $^3J_{HH}$ = 6 Hz, $^4J_{HH}$ = 2 Hz, $^5J_{HH}$ = 1 Hz, 2H, 6-dpk), 8.25

dx.doi.org/10.1021/om400390e | *Organometallics* 2013, 32, 3903−3913

(td, $^3J_{HH}$ = 8 Hz, $^4J_{HH}$ = 2 Hz, 2H, 4-dpk), 8.14 (ddd, $^3J_{HH}$ = 8 Hz, $^3J_{HH}$ = 2 Hz, $^5J_{HH}$ = 1 Hz, 2H, 3-dpk), 7.59 (ddd, $^3J_{HH}$ = 8 Hz, $^3J_{HH}$ = 6 Hz, $^4J_{HH}$ = 2 Hz, 2H, 5-dpk), 7.28 (dd, $^3J_{HH}$ = 8 Hz, $^4J_{HH}$ = 2 Hz, $^3J_{PtH}$ = 71 Hz Pt satellites, 4H, H^o-Ph), 6.77 (t, $^3J_{HH}$ = 7 Hz, 4H, H^m-Ph), 6.65 (tt, $^3J_{HH}$ = 7 Hz, $^4J_{HH}$ = 2 Hz, 2H, H^p-Ph). ^{13}C NMR (125 MHz, CD_2Cl_2): δ 189.4 (CO-dpk), 153.3, 152.1, 143.9, 138.8, 138.4, 128.4, 127.1, 125.9, 122.4 (dpk and Ph aromatic). Anal. Calcd for $PtN_2OC_{23}H_{18}$: C, 51.80; H, 3.41; N, 5.25. Found: C, 51.70; H, 3.54; N, 5.21.

(dpa)PtPh$_2$ ***(3b)***. The ligand was bis(2-pyridyl)amine (dpa). Isolated yield: 0.16 g (84%). ^{1}H NMR (500 MHz, acetone-d_6): δ 9.51 (s, 1H, NH-dpa), 8.06 (dd, $^3J_{HH}$ = 6 Hz, $^4J_{HH}$ = 2 Hz, 2H, 6-dpa), 7.82 (ddd, $^3J_{HH}$ = 8 Hz, $^3J_{HH}$ = 7 Hz, $^4J_{HH}$ = 2 Hz, 2H, 4-dpa), 7.39 (dd, $^3J_{HH}$ = 8 Hz, $^4J_{HH}$ = 2 Hz, $^3J_{PtH}$ = 70 Hz Pt satellites, 4H H^o-Ph), 7.27 (d, $^3J_{HH}$ = 8 Hz, 2H, 3-dpa), 6.76 (t, $^3J_{HH}$ = 8 Hz, 4H, H^m-Ph), 6.72 (ddd, $^3J_{HH}$ = 7 Hz, $^3J_{HH}$ = 6 Hz, $^4J_{HH}$,= 2 Hz, 2H, 5-dpa), 6.62 (t, $^3J_{HH}$ = 7 Hz, 2H, H^p-Ph). ^{13}C NMR (201 MHz, acetone-d_6): δ 152.4, 151.1, 146.7, 139.5, 139.4, 127.2, 121.6, 119.0, 114.7. Anal. Calcd for $PtN_3C_{22}H_{19}$: C, 50.76; H, 3.69; N, 8.07. Found: C, 50.97; H, 3.79; N, 7.90.

(dpo)PtPh$_2$ ***(3c)***. The ligand was bis(2-pyridyl) ether (dpo). Isolated yield: 0.14 g (93%). ^{1}H NMR (300 MHz, CD_2Cl_2): δ 8.19 (d, $^3J_{HH}$ = 6 Hz, $^3J_{PtH}$ = 25 Hz Pt satellite, 2H, H^6-dpo), 7.94 (t, $^3J_{HH}$ = 8 Hz, 2H, H^4-dpo), 7.42 (m, 6H, H^o-Ph and H^3-dpo), 7.06 (t, $^3J_{HH}$ = 7 Hz, 2H, H^5-dpo), 6.91 (t, $^3J_{HH}$ = 7 Hz, 4H, H^m-Ph), 6.79 (t, $^3J_{HH}$ = 7 Hz, 2H, H^p-Ph). ^{13}C NMR (75 MHz, CD_2Cl_2): δ 159.1, 150.0, 143.7, 141.4, 138.5, 127.2, 123.1, 122.0, 115.9 (dpo and Ph aromatic). Anal. Calcd for $PtON_2C_{22}H_{18}$: C, 50.67; H, 3.49; N, 5.37. Found: C, 50.68; H, 3.56; N, 5.21.

General Procedure for the Synthesis of [(N∼N)Pt(Ph)(THF)][BAr′$_4$] Complexes (2b−e and 4a−c). A solution/suspension of (N∼N)Pt(Ph)$_2$ in THF (30 mL) was cooled to approximately −70 °C. One equivalent of $[H(Et_2O)_2][BAr'_4]$ dissolved in THF (∼10 mL, −70 °C) was added. The solution was immediately placed under vacuum, and the volatiles were removed. The residue was treated with *n*-pentane (∼2 mL), which was then removed under vacuum to afford a solid. The solid was dried in vacuo.

Spectroscopic Data for the [BAr′$_4$] Anion. The resonances for the BAr′$_4$ anion demonstrate negligible differences in chemical shift among the complexes. Therefore, for simplicity the NMR data for the anion are given here. ^{1}H NMR (300 MHz, CD_2Cl_2): δ 7.72 (s, 8H, H^o-BAr′$_4$), 7.56 (s, 4H, H^p-BAr′$_4$). ^{13}C NMR (75 MHz, CD_2Cl_2): δ 162.3 (q, Ar′, $^1J_{B\text{-}Cipso}$ = 49 Hz), 135.4 (Ar′), 129.5 (q, *m*-Ar′, $^2J_{C-F}$ = 32 Hz), 125.2 (q, Ar′, $^2J_{C-F}$ = 272 Hz), 118.1 (Ar′). ^{19}F NMR (282 MHz, CD_2Cl_2): δ −63.1 (s, CF_3-Ar′).

[(Me-dpm)Pt(Ph)(THF)][BAr′$_4$] ***(2b)***. Isolated yield: 0.14 g (93%). ^{1}H NMR (800 MHz, CD_2Cl_2): δ 8.56 (d, $^3J_{HH}$ = 6 Hz, 1H, 6-dpm), 7.90 (td, $^3J_{HH}$ = 8 Hz, $^3J_{HH}$ = 2 Hz, 1H, 4-dpm), 7.69 (t, $^3J_{HH}$ = 8 Hz, 1H, 4-dpm), 7.63 (d, $^3J_{HH}$ = 8 Hz, 1H, 3-dpm), 7.48 (t, $^3J_{HH}$ = 7 Hz, 1H, 5-dpm), 7.42 (d, $^3J_{HH}$ = 8 Hz, 1H, 3-dpm), 7.08 (d, $^3J_{HH}$ = 8.0 Hz, 1H, 5-dpm), 6.99−6.90 (m, 5H, Ph), 5.55 (d, $^2J_{HH}$ = 15 Hz, 1H, dpm-CH_2), 4.44 (d, $^3J_{HH}$ = 15 Hz, 1H, dpm-CH_2), 4.17 (m, 2H, α-THF), 3.98 (m, 2H, α-THF), 2.55 (s, 3H, dpm-Me), 1.88 (m, 4H, β-THF). ^{13}C NMR (201 MHz, CD_2Cl_2): δ 165.2, 157.3, 154.2, 150.8, 140.6, 134.0, 136.1, 127.4, 126.1, 125.9, 125.3, 125.2, 123.4 (Me-dpm and Ph aromatic), 77.2 (α-THF), 48.3 (dpm-CH_2), 29.1 (β-THF), 25.4 (dpm-Me), remaining aromatic resonance obscured due to broadening or coincidental overlap. Anal. Calcd for $PtN_2OBF_{24}C_{54}H_{37}$: C, 46.60; H, 2.69; N, 2.01. Found: C, 46.51; H, 2.70; N, 2.07.

[(Me$_2$-dpm)Pt(Ph)(THF)][BAr′$_4$] ***(2c)***. Isolated yield: 0.18 g (95%). ^{1}H NMR (300 MHz, CD_2Cl_2): δ 7.76 (t, $^3J_{HH}$ = 8 Hz, 1H, 4-dpm), 7.64 (t, $^3J_{HH}$ = 8 Hz, 1H, 4-dpm), 7.46 (d, $^3J_{HH}$ = 8 Hz, 1H, 3-dpm), 7.38 (d, $^3J_{HH}$ = 8 Hz, 1H, 5-dpm), 7.33 (d, $^3J_{HH}$ = 8 Hz, 1H, 3-dpm), 7.12 (d, $^3J_{HH}$ = 7 Hz, 2H, H^o-Ph), 7.04 (d, $^3J_{HH}$ = 8 Hz, 1H, 5-dpm), 7.02−6.86 (m, 3H, H^m and H^p-Ph), 5.82 (d, $^2J_{HH}$ = 15 Hz, 1H, dpm-CH_2), 4.48 (d, $^2J_{HH}$ = 15 Hz, 1H, dpm-CH_2), 3.92 (m, 4H, α-THF), 2.94 (s, 3H, dpm-Me), 2.67 (s, 3H, dpm-Me), 1.73 (m, 4H, β-THF). ^{13}C NMR (201 MHz, CD_2Cl_2): δ 164.7, 160.8, 157.5, 154.0, 140.5, 139.9, 137.2, 128.7, 127.4, 125.8, 125.5, 125.3, 123.38, 123.34 (Me$_2$-dpm and Ph aromatic), 76.6 (α-THF), 48.4 (dpm-CH_2), 28.7 (dpm-Me), 24.8 (β-THF), 24.5 (dpm-Me). Anal. Calcd for $PtN_2OBF_{24}C_{54}H_{37}$: C, 46.99; H, 2.80; N, 1.99. Found: C, 46.79; H, 2.76; N, 2.05.

[(Me$_2$-bpy)Pt(Ph)(THF)][BAr′$_4$] ***(2d)***. Isolated yield: 0.13 g (91%). ^{1}H NMR (300 MHz, CD_2Cl_2): δ 8.09−7.79 (m, 4H, bpy), 7.51 (d, $^3J_{HH}$ = 7 Hz, 1H, bpy), 7.17 (m, 3H, bpy and H^o-Ph), 6.98 (m, 3H, H^m and H^p-Ph), 3.96 (m, 4H, α-THF), 2.66 (s, 3H, bpy-Me), 2.05 (s, 3H, bpy-Me), 1.70 (m, 4H, β-THF). ^{13}C NMR (125 MHz, CD_2Cl_2): δ 167.0, 160.7, 159.3, 155.7, 140.2, 139.8, 137.0, 128.7, 128.4, 128.0, 127.5, 125.5, 120.6, 120.3 (bpy and Ph aromatic), 76.2 (α-THF), 29.1 (bpy-Me), 24.7 (β-THF), 23.7 (bpy-Me). Anal. Calcd for $PtN_2OBF_{24}C_{54}H_{37}$: C, 46.60; H, 2.69; N, 2.01. Found: C, 46.18; H, 2.52; N, 1.92.

[(dpe)Pt(Ph)(THF)][BAr′$_4$] ***(2e)***. Isolated yield: 0.12 g (89%). ^{1}H NMR (500 MHz, CD_2Cl_2): δ 8.69 (d, $^3J_{HH}$ = 6 Hz, 1H, 6-dpe), 8.52 (d, $^3J_{HH}$ = 6 Hz, 1H, 6-dpe), 7.69 (m, 10H, H^o-Ar′ and 4-dpe), 7.56 (s, 4H, H^p-Ar′), 7.33 (m, 5H, H^o-Ph, 3-dpe and 5-dpe), 7.02 (t, $^3J_{HH}$ = 7 Hz, 3H, H^m-Ph and 5-dpe), 6.91 (t, $^3J_{HH}$ = 7 Hz, 1H, H^p-Ph), 3.88 (br m, 8H, dpe-CH_2 and α-THF), 1.77 (s, 4H, β-THF). ^{13}C NMR (125 MHz, CD_2Cl_2): δ 162.5, 159.8, 153.4, 150.8, 139.5, 139.4, 136.6, 130.5, 128.7, 127.8, 126.3, 125.2, 124.8, 124.0 (dpe and Ph aromatic), 77.3 (α-THF), 36.16 (dpe-CH_2), 34.07 (dpe-CH_2), 25.08 (β-THF). Anal. Calcd for $PtN_2OBF_{24}C_{54}H_{37}$: C, 46.60; H, 2.69; N, 2.01. Found: C, 46.85; H, 2.81; N, 2.14.

[(dpk)Pt(Ph)(THF)][BAr′$_4$] ***(4a)***. Isolated yield: 0.22 g (92%). ^{1}H NMR (300 MHz, CD_2Cl_2): δ 8.63 (d, $^3J_{HH}$ = 6 Hz, 1H, dpk), 8.33 (d, $^3J_{HH}$ = 6 Hz, 1H, dpk), 8.24 (td, $^3J_{HH}$ = 8 Hz, $^4J_{HH}$ = 2 Hz, 1H, dpk), 8.10 (m, 2H, dpk), 7.85 (m, 10H, H^o-BAr′ and dpk), 7.63 (s, 4H, H^p-BAr′), 7.37 (m, 3H, dpk and H^o-Ph), 7.11 (m, 3H, H^m- and H^p-Ph), 4.06 (m, 4H, α-THF), 1.78 (m, 4H, β-THF). ^{13}C NMR (126 MHz, CD_2Cl_2): δ 185.8 (CO-dpk), 154.6, 153.3, 150.8, 149.3, 141.4, 141.1, 136.1, 130.2, 128.6, 128.5, 127.0 (dpk and Ph aromatic), 77.8 (α-THF), 24.9 (β-THF), remaining three aromatic resonances obscured due to broadening or coincidental overlap. Anal. Calcd for $PtN_2O_2BF_{24}C_{53}H_{33}$: C, 45.74; H, 2.39; N, 2.01. Found: C, 45.76; H, 2.57; N, 2.15.

[(dpa)Pt(Ph)(THF)][BAr′$_4$] ***(4b)***. Isolated yield: 0.19 g (95%). ^{1}H NMR (800 MHz, CD_2Cl_2): δ 8.20 (dd, $^3J_{HH}$ = 6 Hz, $^4J_{HH}$ = 2 Hz, 1H, dpa), 8.11 (dd, $^3J_{HH}$ = 6 Hz, $^4J_{HH}$ = 2 Hz, 1H, dpa), 8.06 (s, 1H, NH-dpa), 7.88 (ddd, $^3J_{HH}$ = 8 Hz, $^3J_{HH}$ = 7 Hz, $^4J_{HH}$ = 2 Hz, 1H, dpa), 7.74 (m, 9H, H^o-BAr′ and dpa), 7.56 (s, 4H, H^p-BAr′), 7.36 (dd, $^3J_{HH}$ = 8 Hz, $^4J_{HH}$ = 2 Hz, 2H, H^o-Ph), 7.18 (ddd, $^3J_{HH}$ = 7 Hz, $^3J_{HH}$ = 6 Hz, $^4J_{HH}$ = 1 Hz, 1H, dpa), 7.13 (d, $^3J_{HH}$ = 8 Hz, 1H, dpa), 7.07 (t, $^3J_{HH}$ = 8 Hz, 2H, H^m-Ph), 6.98 (m, 2H, H^p-Ph and dpa), 6.65 (ddd, $^3J_{HH}$ = 7 Hz, $^3J_{HH}$ = 6 Hz, $^4J_{HH}$ = 1 Hz, 1H, dpa), 4.01 (m, 4H, α-THF), 1.73 (m, 4H, β-THF). ^{13}C NMR (201 MHz, CD_2Cl_2): δ 153.4, 151.7, 149.7, 146.1, 141.2, 141.0, 136.4, 128.3, 125.3, 120.7, 119.8, 115.5, 114.4 (dpa and Ph aromatic), 77.2 (α-THF), 24.9 (β-THF), remaining aromatic resonance obscured due to broadening or coincidental overlap. Anal. Calcd for $PtN_3OBF_{24}C_{52}H_{34}$: C, 45.30; H, 2.49; N, 3.05. Found: C, 45.45; H, 2.63; N, 3.03.

[(dpo)Pt(Ph)(THF)][BAr′$_4$] ***(4c)***. Isolated yield: 0.12 g (98%). ^{1}H NMR (500 MHz, CD_2Cl_2): δ 8.25 (dd, $^3J_{HH}$ = 6 Hz, $^4J_{HH}$ = 2 Hz, 1H, dpo), 8.22 (dd, $^3J_{HH}$ = 6 Hz, $^4J_{HH}$ = 2 Hz, 1H, dpo), 8.11 (td, $^3J_{HH}$ = 8 Hz, $^4J_{HH}$ = 2 Hz, 1H, dpo), 7.99 (td, $^3J_{HH}$ = 8 Hz, $^4J_{HH}$ = 2 Hz, 1H, dpo), 7.72 (s, 8H, H^o-Ar′), 7.54 (m, 5H, H^p-Ar′ and dpo), 7.50 (ddd, $^3J_{HH}$ = 7 Hz, $^3J_{HH}$ = 6 Hz, $^4J_{HH}$ = 1 Hz, 1H, dpo), 7.39 (m, 3H, H^o-Ph and dpo), 7.11 (t, $^3J_{HH}$ = 8 Hz, 2H, H^m-Ph), 7.02 (m, 2H, H^p-Ph and dpo), 4.09 (m, 4H, α-THF), 1.77 (m, 4H, β-THF). ^{13}C NMR (125 MHz, CD_2Cl_2): δ 157.6, 152.9, 146.6, 144.1, 143.8, 136.1, 128.7, 128.5, 125.8, 124.5, 123.9, 117.5, 116.6 (dpo and Ph aromatic), 77.9 (α-THF), 24.9 (β-THF), remaining aromatic resonances obscured due to broadening or coincidental overlap. Anal. Calcd for $PtN_2O_2BF_{24}C_{52}H_{33}$: C, 45.26; H, 2.42; N, 2.03. Found: C, 45.00; H, 2.38; N, 2.15.

Catalytic Olefin Hydroarylation. A representative catalytic reaction is described. [(Me-dpm)Pt(Ph)(THF)][BAr′$_4$] (**2b**; 0.019 g, 0.013 mmol) was dissolved in 12.0 mL of benzene containing 0.01

dx.doi.org/10.1021/om400390e | *Organometallics* 2013, 32, 3903−3913

mol % of hexamethylbenzene (HMB) relative to benzene as an internal standard. The reaction mixture was placed in a stainless steel pressure reactor, and the reactor was charged with ethylene (1.0 bar), pressurized to a total of 7.5 bar with N_2, and heated to 100 °C. After a given duration, the reaction mixture was cooled to room temperature and analyzed by GC/MS. Peak areas of the products and the internal standard were used to calculate product yields. Ethylbenzene production was quantified using linear regression analysis of gas chromatograms of standard samples. A set of five known standards was prepared consisting of 2:1, 4:1, 6:1, 8:1, and 10:1 molar ratios of ethylbenzene to HMB in benzene. A plot of the peak area ratios versus molar ratios gave a regression line. For the GC/MS system, the slope and correlation coefficient (R^2) for ethylbenzene were 0.68 and 0.99, respectively. Identical procedures were used to quantify the production of styrene, 1,3-diethylbenzene, 1,4-diethylbenzene, and 1,2-diethylbenzene. The slope and correlation coefficients (R^2) for these species are respectively as follows: 0.51, 0.99; 0.52, 0.99; 0.53, 0.99; 0.55, 0.99.

■ ASSOCIATED CONTENT

Supporting Information

Text, figures, and CIF files giving details of the kinetic analysis of catalyst decomposition and X-ray structures. This material is available free of charge via the Internet at http://pubs.acs.org.

■ AUTHOR INFORMATION

Corresponding Author

*E-mail: tbg7h@virginia.edu (T.B.G.); t@unt.edu (T.R.C.).

Notes

The authors declare no competing financial interest.

■ ACKNOWLEDGMENTS

T.B.G. and T.R.C. acknowledge The Office of Basic Energy Sciences, U.S. Department of Energy, for support of this work (grant numbers DE-SC0000776 and DE-FG02-03ER15387, respectively). T.B.G. acknowledges the National Science Foundation for the purchase of X-ray diffraction instrumentation at the University of Virginia (CHE-1126602). R.H.C. and T.M. thank Gary Brudvig for useful discussions and also the Office of Basic Energy Sciences, U.S. Department of Energy, for support under DE-PS02-08ER15944 (bis(2-pyridyl) ether synthesis). B.A.M. thanks Benjamin Vaughan for assistance in refinement of X-ray diffraction data.

■ REFERENCES

(1) (a) Goldman, A. S.; Goldberg, K. I., Organometallic C-H Bond Activation: An Introduction. In *Activation and Functionalization of C-H Bonds*; Goldberg, K. I., Goldman, A. S., Eds. American Chemical Society: Washington, DC, 2004; ACS Symposium Series *885*, pp 1−43. (b) Goj, L. A.; Gunnoe, T. B. *Curr. Org. Chem.* **2005**, *9*, 671−685.

(2) (a) Olah, G. A.; Molnar, A., *Hydrocarbon Chemistry*; Wiley-Interscience: New York, 1995. (b) Perego, C.; Ingallina, P. *Catal. Today* **2002**, *73*, 3−22. (c) Perego, C.; Pollesel, P. In *Advances in Nanoporous Materials*; Stefan, E., Ed.; Elsevier: Amsterdam, 2010; Vol. *1*, Chapter 2 (Advances in Aromatics Processing Using Zeolite Catalysts), pp 97−149.

(3) (a) Patinkin, S. H.; Friedman, B. S. Alkylation of Aromatics with Alkenes and Alkanes. In *Friedel-Crafts and Related Reactions*; Olah, G. A., Ed.; Wiley: New York, 1964; Vol. *2*, pp 1−288. (b) Roberts, R. M.; Khalaf, A. A. *Friedel-Crafts Alkylation Chemistry: A Century of Discovery*. Marcel Dekker: New York, 1984.

(4) (a) Foley, N. A.; Lee, J. P.; Ke, Z.; Gunnoe, T. B.; Cundari, T. R. *Acc. Chem. Res.* **2009**, *42*, 585−597. (b) Andreatta, J. R.; McKeown, B. A.; Gunnoe, T. B. *J. Organomet. Chem.* **2011**, *696*, 305−315.

(5) Marcilly, C. Main Acids, Superacids and Bases of Interest in Catalysis. In *Acido-Basic Catalysis*; Editions Technip: Paris, France, 2006; Vol. *2*, pp 515−534.

(6) (a) Murai, S.; Kakiuchi, F.; Sekine, S.; Tanaka, Y.; Kamatani, A.; Sonoda, M.; Chatani, N. *Pure App. Chem.* **1994**, *66*, 1527−1534. (b) Fujii, N.; Kakiuchi, F.; Chatani, N.; Murai, S. *Chem. Lett.* **1996**, *25*, 939−940. (c) Yoshikai, N. *Synlett* **2011**, *2011*, 1047−1051. (d) Gao, K.; Yoshikai, N. *J. Am. Chem. Soc.* **2010**, *133*, 400−402. (e) Harada, H.; Thalji, R. K.; Bergman, R. G.; Ellman, J. A. *J. Org. Chem.* **2008**, *73*, 6772−6779. (f) Miura, M.; Tsuda, T.; Satoh, T.; Nomura, M. *Chem. Lett.* **1997**, *26*, 1103−1104. (g) Murai, S.; Kakiuchi, F.; Sekine, S.; Tanaka, Y.; Kamatani, A.; Sonoda, M.; Chatani, N. *Nature* **1993**, *366*, 529−531. (h) Lewis, L. N.; Smith, J. F. *J. Am. Chem. Soc.* **1986**, *108*, 2728−2735.

(7) (a) Dyker, G.; Muth, E.; Hashmi, A. S. K.; Ding, L. *Adv. Synth. Catal.* **2003**, *345*, 1247−1252. (b) Dorta, R.; Togni, A. *Chem. Commun.* **2003**, 760−761. (c) Youn, S. W.; Pastine, S. J.; Sames, D. *Org. Lett.* **2004**, *6*, 581−584. (d) Thalji, R. K.; Ellman, J. A.; Bergman, R. G. *J. Am. Chem. Soc.* **2004**, *126*, 7192−7193. (e) Tan, K. L.; Bergman, R. G.; Ellman, J. A. *J. Am. Chem. Soc.* **2001**, *123*, 2685−2686. (f) Tan, K. L.; Bergman, R. G.; Ellman, J. A. *J. Am. Chem. Soc.* **2002**, *124*, 13964−13965. (g) Jia, C.; Piao, D.; Oyamada, J.; Lu, W.; Kitamura, T.; Fujiwara, Y. *Science* **2000**, *287*, 1992−1995.

(8) (a) Bhalla, G.; Bischof, S. M.; Ganesh, S. K.; Liu, X. Y.; Jones, C. J.; Borzenko, A.; Tenn, W. J., III; Ess, D. H.; Hashiguchi, B. G.; Lokare, K. S.; Leung, C. H.; Oxgaard, J.; Goddard, W. A., III; Periana, R. A. *Green Chem.* **2011**, *13*, 69−81. (b) McKeown, B. A.; Foley, N. A.; Lee, J. P.; Gunnoe, T. B. *Organometallics* **2008**, *27*, 4031−4033. (c) Luedtke, A. T.; Goldberg, K. I. *Angew. Chem.* **2008**, *120*, 7808−7810. (d) Karshtedt, D.; Bell, A. T.; Tilley, T. D. *Organometallics* **2004**, *23*, 4169−4171. (e) Joslin, E. E.; McMullin, C. L.; Gunnoe, T. B.; Cundari, T. R.; Sabat, M.; Myers, W. H. *Organometallics* **2012**, *31*, 6851−6860. (f) Lail, M.; Arrowood, B. N.; Gunnoe, T. B. *J. Am. Chem. Soc.* **2003**, *125*, 7506−7507. (g) Lail, M.; Bell, C. M.; Conner, D.; Cundari, T. R.; Gunnoe, T. B.; Petersen, J. L. *Organometallics* **2004**, *23*, 5007−5020. (h) Foley, N. A.; Lail, M.; Lee, J. P.; Gunnoe, T. B.; Cundari, T. R.; Petersen, J. L. *J. Am. Chem. Soc.* **2007**, *129*, 6765−6781. (i) Foley, N. A.; Lail, M.; Gunnoe, T. B.; Cundari, T. R.; Boyle, P. D.; Petersen, J. L. *Organometallics* **2007**, *26*, 5507−5516. (j) Foley, N. A.; Ke, Z.; Gunnoe, T. B.; Cundari, T. R.; Petersen, J. L. *Organometallics* **2008**, *27*, 3007−3017.

(9) (a) Oxgaard, J.; Periana, R. A.; Goddard, W. A., III *J. Am. Chem. Soc.* **2004**, *126*, 11658−11665. (b) McKeown, B. A.; Gonzalez, H. E.; Friedfeld, M. R.; Gunnoe, T. B.; Cundari, T. R.; Sabat, M. *J. Am. Chem. Soc.* **2011**, *133*, 19131−19152. (c) McKeown, B. A.; Gonzalez, H. E.; Gunnoe, T. B.; Cundari, T. R.; Sabat, M. *ACS Catal.* **2013**, *3*, 1165−1171. (d) McKeown, B. A.; Gonzalez, H. E.; Friedfeld, M. R.; Brosnahan, A. M.; Gunnoe, T. B.; Cundari, T. R.; Sabat, M. *Organometallics* **2013**, *32*, 2857−2865.

(10) (a) Lersch, M.; Tilset, M. *Chem. Rev.* **2005**, *105*, 2471−2526. (b) Johansson, L.; Tilset, M.; Labinger, J. A.; Bercaw, J. E. *J. Am. Chem. Soc.* **2000**, *122*, 10846−10855. (c) Bercaw, J. E.; Labinger, J. A.; Zhong, H. A. *Abstr. Pap. Am. Chem. Soc.* **2001**, *222*, U412−U413. (d) Parmene, J.; Ivanovic-Burmazovic, I.; Tilset, M.; van Eldik, R. *Inorg. Chem.* **2009**, *48*, 9092−9103.

(11) (a) Strömberg, S.; Zetterberg, K.; Siegbahn, P. E. M. *J. Chem. Soc., Dalton Trans.* **1997**, *22*, 4147−4152. (b) van Gemert, J. T.; Wilkinson, P. R. *J. Phys. Chem.* **1964**, *68*, 645−647. (c) Hartley, F. R. *Chem. Rev.* **1969**, *69*, 799−844. (d) MacDonald, M. G.; Kostelansky, C. N.; White, P. S.; Templeton, J. L. *Organometallics* **2006**, *25*, 4560−4570.

(12) (a) Bowring, M. A.; Bergman, R. G.; Tilley, T. D. *Organometallics* **2011**, *30*, 1295−1298. (b) Karshtedt, D.; McBee, J. L.; Bell, A. T.; Tilley, T. D. *Organometallics* **2006**, *25*, 1801−1811.

(13) (a) Bonnington, K. J.; Zhang, F.; Moustafa, M. M. A. R.; Cooper, B. F. T.; Jennings, M. C.; Puddephatt, R. J. *Organometallics* **2012**, *31*, 306−317. (b) Zhang, F. B.; Prokopchuk, E. M.; Broczkowski, M. E.; Jennings, M. C.; Puddephatt, R. J. *Organometallics* **2006**, *25*, 1583−1591. (c) Zhang, F. B.; Kirby, C. W.; Hairsine, D. W.; Jennings, M. C.; Puddephatt, R. J. *J. Am. Chem. Soc.* **2005**, *127*, 14196−14197.

(14) Ong, C. M.; Jennings, M. C.; Puddephatt, R. J. *Can. J. Chem.* **2003**, *81*, 1196−1205.
(15) Safa, M.; Jennings, M. C.; Puddephatt, R. J. *Organometallics* **2011**, *30*, 5625−5635.
(16) (a) Szuromi, E.; Sharp, P. R. *Organometallics* **2006**, *25*, 558−559. (b) Thomas, J. C.; Peters, J. C. *J. Am. Chem. Soc.* **2001**, *123*, 5100−5101.
(17) McKeown, B. A.; Gonzalez, H. E.; Friedfeld, M. R.; Brosnahan, A. M.; Gunnoe, T. B.; Cundari, T. R.; Sabat, M. *Organometallics* **2013**, *32*, 2857−2865.
(18) Hancock, R. D.; Martell, A. E. *Chem. Rev.* **1989**, *89*, 1875−1914.
(19) Olah, G. A. *Acc. Chem. Res.* **1971**, *4*, 240−248.
(20) Brookhart, M.; Grant, B.; Volpe, A. F. *Organometallics* **2002**, *11*, 3920−3922.
(21) Steele, B. R.; Vrieze, K. *Transition Met. Chem.* **1977**, *2*, 140−144.
(22) Vedernikov, N.; Miftakhov, R.; Borisoglebski, S. V.; Caulton, K. G.; Solomonov, B. N. *Chem. Heterocycl. Compd.* **2002**, *38*, 406−416.
(23) Quagliotto, P.; Viscardi, G.; Barolo, C.; Barni, E.; Bellinvia, S.; Fisicaro, E.; Compari, C. *J. Org. Chem.* **2003**, *68*, 7651−7660.
(24) Hodges, A. S.; Lee, S. Y.; Hardcastle, K. I.; Saadein, M. R.; Eichler, J. F. *Inorg. Chim. Acta* **2011**, *368*, 252−256.